



Available online at www.sciencedirect.com

ScienceDirect

Proceedings
of the
Combustion
Institute

Proceedings of the Combustion Institute 38 (2021) 433-440

www.elsevier.com/locate/proci

Dynamically evaluating mixture effects on multi-channel reactions in flames: A case study for the CH₃ + OH reaction

Lei Lei a, Michael P. Burke b,*

^a Department of Mechanical Engineering, Columbia University, New York, NY 10027, United States
^b Department of Mechanical Engineering, Department of Chemical Engineering, Data Science Institute, Columbia University, New York, NY 10027, United States

Received 7 November 2019; accepted 7 June 2020 Available online 31 August 2020

Abstract

Complex-forming reactions, whose rate constants depend on pressure and collisional energy transfer characteristics of the surrounding bath gas, play a major role in the kinetics of combustion. In most realistic combustion environments, multiple species of distinct collisional energy transfer characteristics are present in significant quantities and thus contribute to collisional energy transfer involved in such systems. Recent studies have indicated that certain representations of multi-component pressure dependence (i.e. "mixture rules") and/or a failure to implement a mixture rule can result in errors reaching an order of magnitude, whereas recently proposed mixture rules yield errors less than 10%. The present study compares the performance of various mixtures rules for representing multi-component pressure dependence of the multi-channel CH₃ + OH reaction in flames, using a novel dynamic procedure for evaluating mixture effects as a function of reaction progress (viz. local temperature, pressure, and mixture composition). This procedure enables mixture effects to be simulated in current combustion codes despite codes not yet having functional forms intended to capture these mixture dependence effects. Results from this procedure, combining master equation simulations and kinetic-transport simulations, indicate that recently proposed mixture rules based on the reduced pressure provide a considerably more accurate representation of mixture effects for CH₃ + OH than previous mixture rules based on the absolute pressure. Furthermore, the present results demonstrate that mixture effects for the CH₃ + OH reaction, which are not accounted for in many models, have a significant effect on predictions of the laminar flame speed – of comparable magnitude to differences motivating parameter adjustments in model development studies.

© 2020 The Combustion Institute. Published by Elsevier Inc. All rights reserved.

Keywords: Mixture rules; Multi-component pressure dependence; Methane flame chemistry

E-mail address: mpburke@columbia.edu (M.P. Burke).

^{*} Corresponding author.

1. Introduction

A large fraction of combustion reactions proceed through rovibrationally excited complexes whose fate is influenced by collisional energy transfer. Indeed, energy-transferring collisions between these excited complexes and the surrounding bath gas are responsible for pressure dependence in combustion kinetics.

Rate constants for these complex-forming reactions depend not only on pressure but also on the bath gas species or, more generally, bath gas mixture composition. Current frameworks for pressure-dependent reactions (e.g. as used in combustion codes [1–4]) are largely premised on theories and data for pure, inert bath gases. In combustion mixtures, however, multiple species are present in sufficient amounts to contribute to energy transfer and, therefore, influence rate constants of pressure-dependent reactions. The effects of mixture composition on pressure-dependent rate constants – if they are treated at all – are usually treated via a "mixture rule," which estimates rate constants in the bath gas mixture from those of the individual components.

Available options for treating mixture effects in combustion codes [1–4] differ among codes, often differ among versions of the same code, and even differ among representations of pressure dependence within the same version of the same code. For reactions expressed using the Troe formula [5] with a single specification of centering factors and Arrhenius expression for the low-pressure limit, along with temperature- and pressure-independent thirdbody efficiencies, it is usually the case that thirdbody efficiencies operate as multipliers on the lowpressure limit rate constant, which is then used to calculate the rate constant at the given pressure in the mixture - yielding a mixture rule (under the limitations of temperature- and pressureindependent third-body efficiencies) equivalent to our more general linear reduced-pressure-based mixture rule (LMR,R in Table 1), which we find to be very effective in representing mixture effects [6–8]. However, the inability to specify unique temperature and pressure dependence for each bath gas, in addition to limitations of the original Troe formula [5] in representing pressure dependence for any bath gas, contribute to potential errors for this option in treating mixture pressure dependence of up to $\sim 90\%$ for even single channel reactions [6]. Furthermore, the need to represent the more complicated pressure dependence of multi-channel and/or multi-well reactions has motivated the use of forms with many more parameters that go beyond forms (such as the Troe formula [5]) based on the simple Lindemann–Hinshelwood form.

For these more complicated pressure-dependent forms (e.g. PLOG and Chebyshev polynomials)

Table 1 Mixture rules for multi-component pressure dependence

$$\begin{split} \operatorname{LMR,P:} &\quad k_{p,LMR,P}(T,P,\underline{X}) = \sum_{i} k_{i,p}(T,P)X_{i} \\ \operatorname{LMR,R:} &\quad k_{p,LMR,R}(T,P,\underline{X}) = \sum_{i} k_{i,p}(T,R_{LMR})\tilde{X}_{i,LMR} \\ &\quad R_{LMR}(T,P,\underline{X}) = \frac{\sum_{i} k_{0,i}(T) \ X_{i}[M]}{k_{\infty}(T)} \\ &\quad \tilde{X}_{i,LMR}(T,P,\underline{X}) = \frac{k_{0,i}(T) \ X_{i}}{\sum_{j} k_{0,j}(T) \ X_{j}} \\ \operatorname{NMR,R:} &\quad k_{p,NMR,R}(T,P,\underline{X}) = \sum_{i} k_{i,p}(T,R_{NMR})\tilde{X}_{i,NMR} \\ &\quad R_{NMR}(T,P,\underline{X}) = \frac{\sum_{i} f_{i}(T,\underline{X}) \ k_{0,i}(T) \ X_{i}[M]}{k_{\infty}(T)} \\ &\quad \tilde{X}_{i,NMR}(T,P,\underline{X}) = \frac{f_{i}(T,\underline{X}) \ k_{0,j}(T) \ X_{i}}{\sum_{j} f_{j}(T,\underline{X}) \ k_{0,j}(T) \ X_{j}} \\ \operatorname{Subscripts} i \ \text{and} \ p \ \text{refer} \ \text{to} \ \text{the} i^{th} \ \text{component} \ \text{and} \ p^{\text{th}} \ \text{reacching} \end{split}$$

tion channel.

that have no inherent limitations on the accuracy of the representation for pressure dependence for a single bath gas nor on the number of channels or wells in the reaction, there are three common possibilities for the way mixture effects are treated in codes. In the first possibility, pressureand temperature-dependent rate constants cannot be specified uniquely for each bath gas. Given that some bath gases have very high third-body efficiencies (e.g. ~ 20 for H₂O in some reactions [9,10]), the inability to specify bath gas dependence of rate constants can be easily understood to give potential errors of an order of magnitude. In the second possibility, pressure- and temperature-dependent rate constants can be specified uniquely for each bath gas species, but each separate reaction expression is assumed to occur independently – i.e. no mixture rule is used. This lack of a mixture rule can be easily understood to give potential errors of up to a factor of n, where n is the number of separate expressions, in the high-pressure limit. In the third possibility, pressure- and temperature-dependent rate constants can be specified uniquely for each bath gas species, and the classic linear mixture rule (LMR,P) in Table 1) is used to estimate the rate constant in the mixture. At first glance, this third possibility may seem to be best of the three, in that it is not clearly in error a priori. However, despite many studies of mixture effects nearly fifty years ago for single-channel reactions [6,11,12], particularly in the low-pressure limit, the classic linear mixture rule had been scarcely tested across the intermediate falloff regime and for multi-channel and/or multi-well reactions.

We have been conducting a series of studies developing and testing representations of mixture effects for multi-channel and/or multi-well reactions using ab initio master equation calculations as a benchmark. To date, we have tested the classic linear mixture rule and two recent mixture

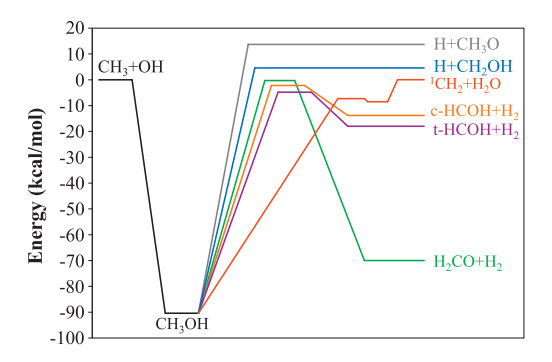


Fig. 1. Potential energy surface for the $CH_3 + OH$ reaction (excluding the abstraction reaction, $CH_3 + OH = {}^3CH_2 + H_2O$) [19].

rules [6-8,13] (cf. Table 1) against master equation calculations for the single-channel H + O₂ $(+M) = HO_2$ (+M) reaction and estimated the corresponding uncertainties due to mixture rules on high-pressure hydrogen flame speed predictions [6] and on experimental determinations of thirdbody efficiencies [13]; we have tested these three mixture rules against master equation calculations for the multi-channel CH₂O decomposition reaction [7] and allyl + HO₂ reaction [8] and calculated the impact of mixture representations for allyl + HO₂ on high-pressure propene ignition delay times [8]. A key finding from our results so far is that the classic linear mixture rule yields errors of up to \sim 60% for single-well, single-channel reactions and a factor of ~ 10 for single-well, multi-channel reactions – such that all three of the possible treatments of mixture effects (for the most accurate and general forms for representing pressure dependence) have the potential to introduce substantial errors in estimating rate constants in mixtures.

We, therefore, have developed new mixture rules for use in combustion codes that represent multicomponent pressure dependence more accurately for our previous test cases and hence provide a promising approach to incorporate mixture effects in combustion codes. We are also pursing additional test cases to ensure the general applicability of these new mixture rules to a wide range of reactions and combustion environments so that they can be used reliably in future combustion modeling software. Our ultimate goal is to develop representations of mixture composition dependence that accurately describe the kinetics of excited complexes undergoing energy-transferring collisions with multiple species [6–8] and reactive collisions [14–18].

In the present study, we assess the impact of mixture effects for multi-channel reactions on laminar flame speed predictions, focusing on the $CH_3 + OH$ reaction (cf. Fig. 1) as a case study. Product-channel-specific rate constants for the $CH_3 + OH$ reactions, and specifically their branch-

ing ratio at high temperatures, were identified as important factors in predicting flame speeds in recent modeling studies [20,21] given their differing effects on the radical pool. As discussed above, currently available representations of multi-component pressure and temperature dependence in combustion codes are limited for multi-channel systems. And for this multi-channel CH₃ + OH reaction, it is common (e.g. [20–24]) for kinetic models to use pressure-dependent rate constants calculated by Jasper et al. [19] for He within representations that assume that rate constants are independent of the bath gas species.

Therefore, the objectives of the present study are to investigate mixture effects on CH₃ + OH at the local mixture and temperature conditions encountered in methane flames at various pressures, assess performance of mixture rules in representing them, and evaluate their impact on laminar flame speed predictions. Below, we first present various mixture rules for representing multi-component pressure dependence, the numerical details for the master equation calculations, and the method for dynamically evaluating mixture effects within freely propagating flame simulations. This novel dynamic procedure enables mixture effects to be simulated in current combustion codes despite codes not yet having functional forms intended to capture these mixture dependence effects. Using this procedure, we then demonstrate the impacts of mixture effects on the CH₃ + OH reaction within methane flames, show their impacts on methane flame speeds, and assess the performance of mixture rules in representing them. Finally, we explore how these effects are influenced by pressure.

The results below suggest that mixture effects are significant in multi-component systems – of comparable magnitude to differences motivating parameter adjustments in model development studies. While the classic linear mixture rule exhibits deficiencies in capturing mixture effects, recently proposed reduced-pressure-based mixture rules are found to provide a reasonable representation of mixture effects. Therefore, their incorporation into combustion codes would be worthwhile.

2. Analytical and computational methods

2.1. Mixture rules

Three mixture rules are considered here (Table 1): the classic linear mixture rule (LMR,P), which is based on absolute pressure (P), and two recently developed mixture rules (LMR,R and NMR,R) based on the reduced pressure (R). The latter two have been shown to better represent mixture behavior for other single-well, single-channel and single-well, multi-channel reactions [6–8].

The classic linear mixture rule (LMR,P), estimates the rate constant of the p^{th} reaction chan-

nel in the mixture, $k_p(T, P, \underline{X})$, as a linear sum of the rate constants of each bath gas component at the same pressure, $k_{i,p}(T, P)$, weighted by their mole fractions, X_i , in the mixture. (Throughout the text, X denotes the vector of mole fractions of each species in the mixture.) The linear mixture rule in reduced pressure (LMR,R) estimates the rate constant of the p^{th} reaction channel in the mixture, $k_p(T, P, \underline{X})$, as a linear sum of the rate constants of each bath gas component evaluated at the same reduced pressure, $k_{i,p}(T, R)$, weighted by each component's fractional contribution to the reduced pressure, \tilde{X}_i . The nonlinear mixture rule in reduced pressure (NMR,R) differs from LMR,R in its additional incorporation of activity coefficients for each component, $f_i(T,$ X), which account for nonlinearities in the lowpressure limit [7,11], in the calculation of the reduced pressure. (A detailed derivation of $f_i(T, X)$ and the procedures to solve for it for each component in a multi-channel system are available in [7].) In each case, the reduced pressure for multi-channel reactions is calculated from the total decomposition low-pressure-limit rate constants in each bath gas component, $k_{0,i}(T)$, rather than the *channel-specific* low-pressure-limit rate constants, $k_{0,i,p}(T)$, since the former better reproduces master equation calculations [7].

2.2. Numerical simulations

2.2.1. Master equation calculations

Master equation calculations were performed using the PAPR-MESS code [25] for the CH₃OH system, with the potential energy surface (Fig. 1) from Jasper et al. [19]. The PAPR-MESS input files were first generated from the original Variflex inputs [19] and confirmed to yield the same rate constants (within 5%). Similar to original calculations in He [19], the standard exponential-down model [11] is used to describe the collisional energy transfer function (using the same average energy transferred per down collision, $\langle \Delta E_d \rangle = 133 \times (T/298 \text{ K})^{0.8} \text{ cm}^{-1}$, for He as [19]); the collision frequency (Z) is estimated using the Lennard-Jones model (using the same parameters, $\sigma = 2.57 \text{ Å}$ and $\epsilon = 7.1 \text{ cm}^{-1}$, for He as [19]).

In the flames considered below, O_2 , N_2 , CO_2 , CH_4 , and H_2O , together with He, comprise over 96% of the local mixture everywhere throughout the simulation domain. Given that data for the relevant bath gases are not available for the CH_3OH system, the present calculations assume third-body efficiencies relative to He, $\mu_{0,i,He} = k_{0,i}/k_{0,He}$, of 1.5, 1.5, 4, 6, and 9 for $i = O_2$, N_2 , CO_2 , CH_4 , and H_2O , respectively, which are within the range of reported values for these bath gases in other reactions [9,10,26]. While non-unity third-body efficiencies usually arise from differences in both Z and $\langle \Delta E_d \rangle$, the results shown below use the same Z for

Table 2 Energy transfer parameters for considered colliders.

	$\langle \Delta E_d \rangle_i (\mathrm{cm}^{-1})$	$\mu_{i,0,A}(T)$	Colliders
	$133.0 \times (T/298)^{0.8}$	1	Не
	$184.1 \times (T/298)^{0.8}$	1.5	O_2 / N_2
	$506.3 \times (T/298)^{0.8}$	4	CO_2
	$992.3 \times (T/298)^{0.8}$	6	CH_4
Collider E	$2296.9 \times (T/298)^{0.8}$	9	H_2O

all bath gases and attribute higher third-body efficiencies solely to higher $\langle \Delta E_d \rangle$ (Table 2) – which we have found to provide the most rigorous tests of the new (more accurate) reduced-pressure-based mixture rules [6,7].

When differences in the third-body efficiencies are instead solely attributed to differences in Z (i.e. using the same $\langle \Delta E_d \rangle$ for all bath gases), both LMR,R and NMR,R exactly reproduce master-equation-calculated rate constants in mixtures (see Supplemental Material). Thus, the performance of new reduced-pressure mixture rules for mixtures with differences in both Z and $\langle \Delta E_d \rangle$ among colliders would likely be at least as good as (and probably better than) indicated in the current paper.

2.2.2. Dynamic procedure for evaluating mixture effects in flames

Laminar flame simulations were performed for ${\rm CH_4/O_2/diluent}$ mixtures using the FreeFlame module in Cantera [1]. The simulations include multi-component transport and Soret effects; the grid is adaptively refined to achieve gradient and curvature values of <0.02 (yielding nearly 1000 grid points).

Model predictions are shown below using various modified versions of the model of Metcalfe et al. [20]. In these various model versions, rate constants for the $CH_3 + OH$ reaction are calculated either from the master equation for pure He as the bath gas (similar to the original calculations [19]), from the master equation for the local mixture as the bath gas, or from each of the three mixture rules for the local mixture as the bath gas.

Calculations based on rate constants from the master equation for He as the bath gas are obtained by directly replacing the rate constants in Metcalfe et al. [20] with Arrhenius fits to rate constants calculated from the master equation with He as the bath gas at each pressure. However, due to current limitations in the ability to represent multicomponent pressure dependence in Cantera and other combustion codes, the other model versions use Arrhenius fits to rate constants calculated using the local mixture composition (obtained from flame simulations) at each temperature for each set of initial conditions. For these model versions for each set of initial conditions, simulations are first performed using the nominal model [20] and then the temperature, T, and mole fractions of major

species, X, (which account for over 96% of the entire mixture) are sampled every five grid points to ensure a thorough coverage of the computational domain. Master equation input files are then generated for each sampling point (where any species other than O₂, N₂, CO₂, CH₄, and H₂O are assumed to have the same energy transfer parameters as He), and the rate constants for each channel at the specific sampling condition, $k_p(T, P, X)$, are calculated using PAPR-MESS code. The resultant rate constants are then fitted to Arrhenius expressions where the temperature dependence of the fit captures the variations in both the local temperature and mixture composition through the flame - thus allowing mixture effects to be simulated in Cantera despite Cantera not having functional forms intended to capture these mixture dependence effects. This procedure is implemented automatically with in-house scripts for each initial equivalence ratio and pressure condition. The procedure used for each mixture rule is the same except that each mixture rule, rather than the master equation, is used to evaluate $k_p(T, P, \underline{X})$ at each condition. Iterations of this procedure were found to yield negligible differences (< 1%) at representative conditions.

3. Results and discussion

3.1. Mixture effects on $CH_3 + OH$ within the flame

The effect of mixture composition on CH_3 + OH reaction rate constants inside a flame is demonstrated in Fig. 2 for a stoichiometric $CH_4/O_2/He$ flame at 10 atm. As shown in Fig. 2a and b, the total CH_3 + OH reaction rate peaks at a location where the temperature is $\sim 2000~K$, the reactants are nearly completely depleted, and the products are present in high mole fractions – with $\sim 4\%~O_2$, $\sim 0\%~CH_4$, $\sim 3\%~CO_2$ and $\sim 13\%~H_2O$.

Overall, throughout the flame, the presence of species with higher third-body efficiencies than He (CH₄, O₂, CO₂, H₂O) in large quantities indicates that the collisional energy transfer rate for the mixture is higher than for pure He. Consequently, as indicated in Fig. 2c, rate constants in the mixture are higher for all stabilization/decomposition channels and lower for all chemically activated channels than in pure He. The enhancements in stabilization rate constants become more pronounced with increasing temperature – as the stabilization reactions approach a pressure falloff regime (i.e. the low pressure limit) where energy transfer is more rate limiting. Similarly, the reductions in the chemically activated rate constants become less pronounced with increasing temperature – as the chemically activated reactions approach a pressure falloff regime where they are independent of energy transfer rates. At the location of peak total $CH_3 + OH$ reaction rates, rate constants are higher than their corre-

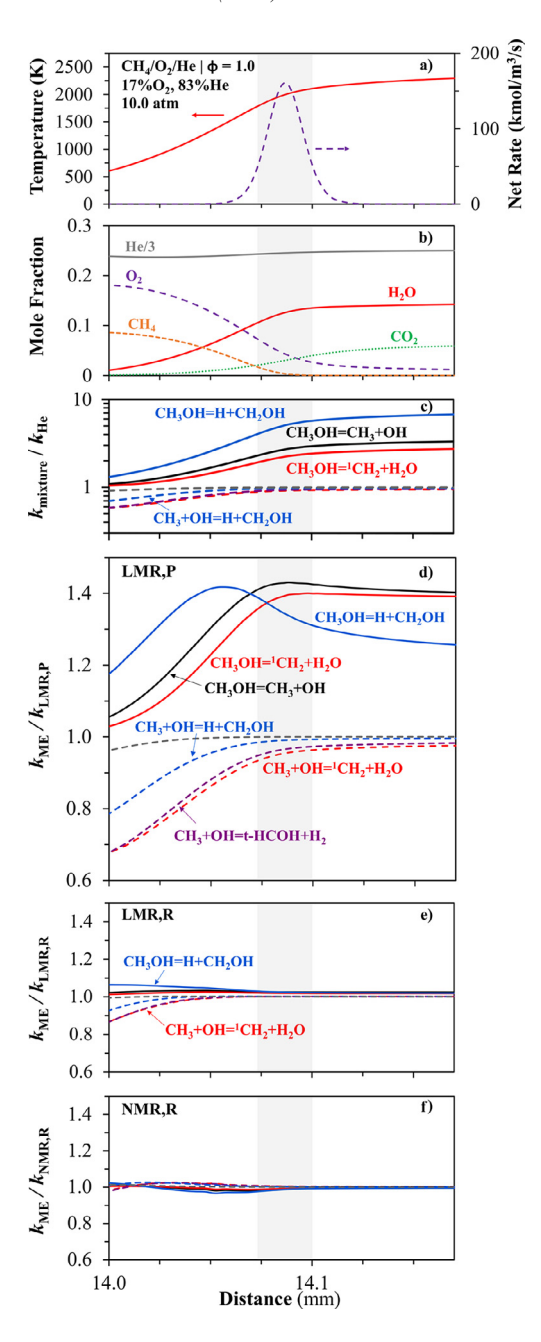


Fig. 2. Simulation results for a stoichiometric $CH_4/O_2/He$ flame at 10.0 atm: a) temperature and net reaction rate of $CH_3 + OH$; b) species profiles; c) ratio of rate constants in the mixture to those in pure He; and deviation of rate constants estimated by d) LMR,P, e) LMR,R, and f) NMR,R from those calculated by the master equation.

sponding values in pure He for stabilization reactions (by a factor of ~ 3 for CH₃ + OH = CH₃OH) though are very close to their corresponding values

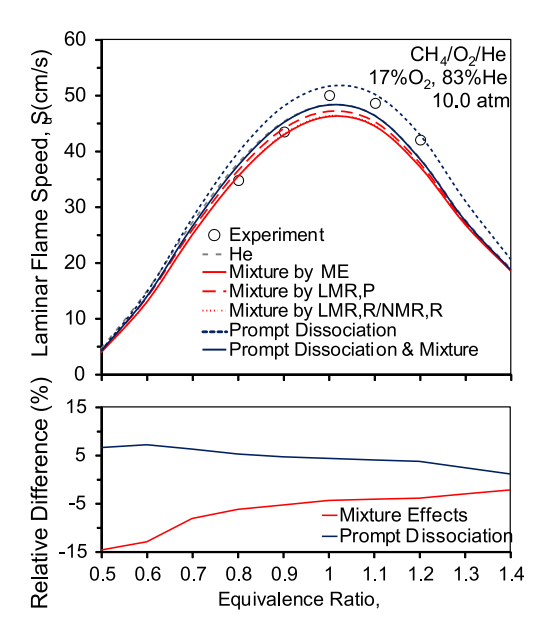


Fig. 3. Laminar flame speeds for $CH_4/O_2/He$ mixtures at 10.0 atm (top) and the relative difference between flame speed predictions with and without mixture effects or prompt dissociation (bottom). Lines show model predictions as indicated in the legend. Symbols show experimental measurements from [27].

in pure He for chemically activated reactions – suggesting that the primary impact of mixture composition on the CH_3 + OH reaction for the flame conditions plotted in Fig. 2 is to increase the stabilization rate

As shown in Fig. 2d, rate constants estimated by the classic linear mixture rule (LMR,P) exhibit deviations from those calculated from the master equation – under-predicting some channels and over-predicting other channels by up to $\sim 40\%$. At the location of peak total CH₃ + OH reaction rates, the deviations for stabilization/decomposition rates are most significant, where rate constants for CH₃ + OH = CH₃OH are under-predicted by LMR,P by $\sim 40\%$. By contrast, as shown in Fig. 2e–f, the reduced-pressure-based mixture rules yield significantly smaller deviations – with maximum deviations of $\sim 10\%$ for LMR,R and $\sim 5\%$ for NMR,R (similar to our results for other reaction systems [6–8]).

3.2. Mixture effects on laminar flame speeds

To demonstrate the impact that mixture effects for the CH₃ + OH reaction have on flame speed predictions, Fig. 3 compares flame speed predictions for CH₄/O₂/He mixtures at 10 atm among various models containing different treatment of mixture

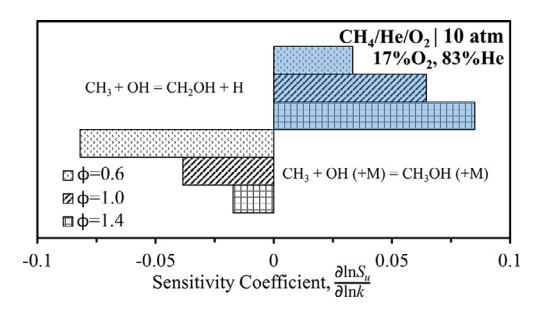


Fig. 4. Sensitivity coefficients of $CH_4/O_2/He$ flame speeds at 10.0 atm to the most sensitive $CH_3 + OH$ rate constants.

effects for the CH_3 + OH reaction. These results indicate that predicted flame speeds using rate constants calculated from the master equation for the mixture are lower than those for pure He – by as much as $\sim 15\%$ at lean conditions.

Sensitivity analysis for these conditions (Fig. 4) indicates that CH₃ + OH = CH₃OH and CH₃ + $OH = CH_2OH + H$ are the two most sensitive CH₃ + OH reaction channels at these flame conditions, where $CH_3 + OH = CH_3OH$ (a chainterminating reaction) inhibits reactivity and CH₃ + OH = CH_2OH + H (a chain-carrying reaction) promotes reactivity. The magnitude of the sensitivity coefficient for CH₃ + OH = CH₃OH, which Fig. 2 shows to be among the channels most strongly affected by mixture composition, is highest at lean conditions, where the largest differences in flame speed predictions are observed among different treatments of mixture effects in Fig. 3. Overall, Fig. 2 indicates that including the effects of local mixture composition on the CH₃ + OH reaction tend to increase stabilization reaction rates (e.g. for $CH_3 + OH = CH_3OH$) and decrease chemically activated reaction rates (e.g. for $CH_3 + OH =$ $CH_2OH + H)$ – both of which tend to reduce the flame speed. As discussed in the previous section, LMR,P underestimates the stabilization rate constants and overestimates the chemically activated rate constants (cf. Fig. 2d). As a result, simulated flame speeds using rate constants from LMR,P for the mixture are higher than those using rate constants from the master equation for the mixture. By contrast, simulations that employ either LMR,R or NMR,R to estimate CH₃ + OH reaction rate constants in the mixture yield predicted flame speeds that are nearly identical to those that employ rate constants directly calculated from the master equation for the mixture.

Additional calculations varying the third-body efficiencies in Table 2 (to evaluate the influence of their uncertainties) indicate that the predicted flame speeds for the mixture could be lower than those for pure He by $\sim 7\%$ (if all $\mu_{0,i,A}$ are lower by a factor of 2) to $\sim 20\%$ (if all $\mu_{0,i,A}$ are higher by

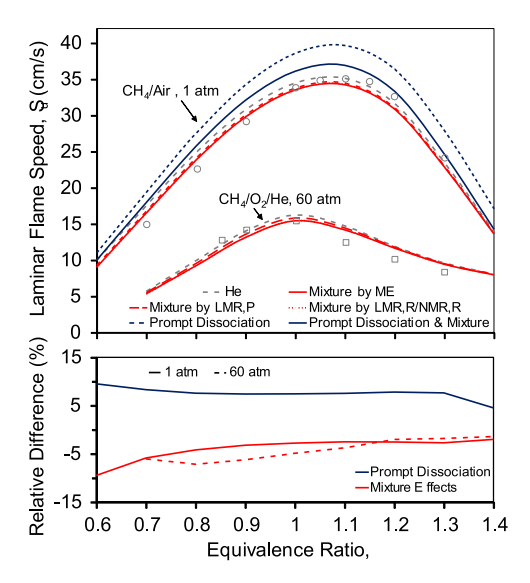


Fig. 5. Laminar flame speeds for CH₄/air mixtures at 1.0 atm and CH₄/O₂/He mixture (15%O₂, 85%He) at 60.0 atm (top) and the relative difference between flame speed predictions with and without mixture effects or prompt dissociation (bottom). Lines show model predictions as indicated in the legend. Symbols show experimental meanurements from [29] (open circles) and from [27] (open squares). (Note: model predictions including prompt dissociation were not performed at 60 atm given that prompt dissociation fractions were not provided at 60 atm in [28].)

a factor of 2) at the lean conditions of Fig. 3 – altogether suggesting that the mixture effects, which cannot yet be directly treated in current kinetic models and codes, comprise a significant source of uncertainty in combustion simulations.

For context, the differences in predicted flame speeds due to mixture effects for CH₃ + OH are of comparable magnitude to the differences between predictions and experimental data motivating parameter adjustments in model development studies [20]. Additional simulations (based on the variant of the model of Metcalfe et al. [20] from Labbe et al. [28]) are also shown in Fig. 3 to explore the extent to which the flame speed reductions from mixture effects may counterbalance flame speed enhancements from HCO prompt dissociation. Interestingly, at near stoichiometric conditions, the impact of mixture effects for $CH_3 + OH$ and HCO prompt dissociation are similar in magnitude though opposite in sign, such that they approximately cancel. However, for leaner mixtures, the impacts of mixture effects on the $CH_3 + OH$ reaction become significantly stronger.

3.3. Mixture effects across various pressures

To assess the impacts of mixture effects for the CH₃ + OH reaction on flame speeds at differ-

ent pressures, flame speed predictions for the same model variants are shown in Fig. 5 for $CH_4/O_2/N_2$ mixtures at 1 atm and for $CH_4/O_2/He$ mixtures at 60 atm. At both 1 atm and 60 atm, simulations using CH_3 + OH rate constants calculated from the master equation for the mixture are lower than simulations using CH_3 + OH rate constants calculated from the master equation assuming pure He as the bath gas – by up to $\sim 10\%$ at 1 atm and $\sim 8\%$ at 60 atm.

Again, simulations employing the classic linear mixture rule to estimate CH₃ + OH rate constants noticeably differ from those employing the master equation to calculate CH₃ + OH rate constants in the mixture. However, simulations employing reduced-pressure-based mixture rules (LMR,R and NMR,R) are nearly identical to those employing the master equation to calculate CH₃ + OH rate constants in the mixture.

4. Conclusions

The performance of various mixture rules representing multi-component pressure dependence for CH₃ + OH was evaluated via comparisons against master equation calculations. Comparisons revealed that the classic linear mixture rule (LMR,P) yields deviations for mixture rate constants of $\sim 40\%$ for typical combustion mixtures, whereas newly proposed mixture rules based on reduced pressure exhibit deviations of generally less than $\sim 10\%$ and $\sim 5\%$ respectively. Flame speed predictions suggest that the impacts of mixture effects for CH₃ + OH are comparable to those motivating rate parameter adjustments in modeling studies to reproduce combustion measurements, and the impacts are as strong as, if not stronger than, those from HCO prompt dissociation for the considered conditions. Newly proposed reducedpressure mixture rules are shown to accurately capture these mixture effects within combustion simulations.

A novel dynamic correction procedure was presented to enable mixture effects to be simulated in current combustion codes despite codes not yet having functional forms intended to capture these mixture dependence effects. Now that this procedure has revealed that mixture effects can be significant and newly proposed mixture rules are capable of representing them, it is recommended that future combustion codes incorporating these validated mixture rules will instead account for such mixture effects directly without the need for the present correction procedure. Similarly, improved quantification of mixture effects for the $CH_3 + OH$ reaction requires improved characterization of energy transfer parameters for various bath gases, including CO₂ and H₂O (in addition to common diluents). Until then, it appears that failure to account for mixture effects could be responsible for flame speed uncertainties as large as 20% – which greatly exceeds typically quoted experimental uncertainties and is comparable to differences between model predictions and experimental data motivating parameter adjustments in modeling studies.

Declaration of Competing Interest

None.

Acknowledgments

The authors gratefully acknowledge support from the National Science Foundation through a grant from the Combustion and Fire Systems program (CBET-1706252) and the Donors of the American Chemical Society Petroleum Research Fund through a Doctoral New Investigator (DNI) award (PRF-56409-DNI-6) and thank Ahren Jasper for sharing input files from [19].

Supplementary material

Supplementary material associated with this article can be found, in the online version, at doi:10. 1016/j.proci.2020.06.187.

References

- D. G. Goodwin, H. K. Moffat, R. L. Speth, Cantera: an object-oriented software toolkie for chemical kinetics, thermodynamics, and transport processes, 2017.
- [2] R. J. Kee, F. M. Rupley, J. A. Miller, Chemkin-II: a fortran chemical kinetics package for the analysis of gas-phase chemical kinetics, 1989.
- [3] A. Cuoci, A. Frassoldati, T. Faravelli, E. Ranzi, Comput. Phys. Commun. 192 (2015) 237–264.
- [4] H. Pitsch, FlameMaster: a C++ computer program for 0D combustion and 1D laminar flame calculations, 1998.
- [5] R.G. Gilbert, K. Luther, J. Troe, Ber. Bunsenges. Phys. Chem. 87 (2) (1983) 169–177.
- [6] M.P. Burke, R. Song, Proc. Combust. Inst. 36 (2017) 245–253.
- [7] L. Lei, M.P. Burke, *J. Phys. Chem. A* 123 (3) (2019) 631–649.
- [8] L. Lei, M.P. Burke, *Proc. Combust. Inst.* 37 (1) (2019) 355–362.

- [9] J.V. Michael, M.-C. Su, J.W. Sutherland, J.J. Carroll, A.F. Wagner, J. Phys. Chem. A 106 (21) (2002) 5297–5313.
- [10] J. Shao, R. Choudhary, A. Susa, D.F. Davidson, R.K. Hanson, *Proc. Combust. Inst.* 37 (2019) 145–152.
- [11] J. Troe, Ber. Bunsenges. Phys. Chem. 84 (1980) 829–834.
- [12] J. Dove, S. Halperin, S. Raynor, J. Chem. Phys. 81 (1984) 799–810.
- [13] L. Lei, M.P. Burke, Combust. Flame 213 (2020) 467–474.
- [14] M.P. Burke, S.J. Klippenstein, *Nat. Chem.* 9 (11) (2017) 1078–1082.
- [15] M.P. Burke, C.F. Goldsmith, Y. Georgievskii, S.J. Klippenstein, Proc. Combust. Inst. 35 (1) (2015) 205–213
- [16] M.C. Barbet, K. McCullough, M.P. Burke, Proc. Combust. Inst. 37 (1) (2019) 347–354.
- [17] A.W. Jasper, R. Sivaramakrishnan, S.J. Klippenstein, J. Chem. Phys. 150 (11) (2019) 114112.
- [18] L. Lei, M.P. Burke, *Proc. Combust. Inst.* (2020) (in press).
- [19] A.W. Jasper, S.J. Klippenstein, L. Harding, B. Ruscic, J. Phys. Chem. A 111 (2007) 3932–3950.
- [20] W.K. Metcalfe, S.M. Burke, S.S. Ahmed, H.J. Curran, Int. J. Chem. Kinet. 45 (10) (2013) 638–645.
- [21] H. Hashemi, J.M. Christensen, S. Gersen, H. Levinsky, S.J. Klippenstein, P. Glarborg, *Combust. Flame* 172 (2016) 349–364.
- [22] C.-W. Zhou, Y. Li, U. Burke, C. Banyon, K.P. Somers, S. Ding, S. Khan, J.W. Hargis, T. Sikes, O. Mathieu, E.L. Petersen, M. AlAbbad, A. Farooq, Y. Pan, Y. Zhang, Z. Huang, J. Lopez, Z. Loparo, S.S. Vasu, H.J. Curran, *Combust. Flame* 197 (2018) 423–438.
- [23] P. Glarborg, J.A. Miller, B. Ruscic, S.J. Klippenstein, Prog. Energy Combust. Sci. 67 (2018) 31–68.
- [24] S.M. Sarathy, P. Oßwald, N. Hansen, K. Kohse-Höinghaus, Prog. Energy Combust. Sci. 44 (2014) 40–102.
- [25] Y. Georgievskii, J.A. Miller, M.P. Burke, S.J. Klippenstein, J. Phys. Chem. A 117 (2013) 12146–12154.
- [26] A.W. Jasper, J.A. Miller, S.J. Klippenstein, J. Phys. Chem. A 117 (47) (2013) 12243–12255.
- [27] D.L. Zhu, C.K. Law, S.D. Tse, Proc. Combust. Inst. 29 (2002) 1461–1469.
- [28] N.J. Labbe, R. Sivaramakrishnan, C.F. Goldsmith, Y. Georgievskii, J.A. Miller, S.J. Klippenstein, *Proc. Combust. Inst.* 36 (1) (2017) 525–532.
- [29] W. Lowry, J. de Vries, M. Krejci, E. Petersen, Z. Serinyel, W. Metcalfe, H. Curran, G. Bourque, J. Eng. Gas Turb. Power 2 (2010) 855–873.